Earth and Planetary Science Letters xxx (2009) xxx–xxx

Contents lists available at ScienceDirect

Earth and Planetary Science Letters

journal homepage: www.elsevier.com/locate/epsl

Earthquake-induced barium anomalies in the Lisan Formation, Dead Sea Rift valley, Israel

Amitai Katz [a,*], Amotz Agnon [a,1], Shmuel Marco [b,2]

[a] The Hebrew University of Jerusalem, Institute of Earth Sciences, Edmond Safra Campus, Givat-Ram, Jerusalem 91904, Israel
[b] Department of Geophysics and Planetary Sciences, Tel Aviv University, Tel Aviv 69978, Israel

ARTICLE INFO

Article history:
Received 13 January 2009
Received in revised form 20 May 2009
Accepted 23 June 2009
Available online xxxx

Editor: L. Stixrude

Keywords:
barium
Dead Sea
seismite
earthquake
Lisan
recurrence rate

ABSTRACT

Prominent barium concentration anomalies that appear within earthquake brecciated layers (seismites) in the late Pleistocene lacustrine Lisan Formation in the Dead Sea Basin (DSB) are described and discussed here for the first time. Chemical analyses of samples from vertical profiles through the seismites display asymmetric Ba concentration peaks. The peaks start a few centimeters above the seismite's base and gradually rise to maxima reaching some 1000 ppm Ba, before falling off to background values (around 100 ppm), or abutting against the upper boundary of the breccia layer.

High resolution SEM and electron microprobe analyses disclose that the Ba in the anomalies resides within prismatic crystallites (mostly<2 μm in length) composed of a $Ba(Sr)SO_4$ mineral (designated "BM" henceforth). These are lacking altogether in the normal (non-seismic) underlying and overlying sediments. The crystallites are much smaller than the adjacent, supporting matrix grains of the gradually-bedded seismite, and show no size-sorting relationship with the latter. The peaks of the anomalies reflect higher population density, rather than larger crystal sizes, of the BM crystallites therein.

Mass balance calculations show that the mass of Ba^{2+} dissolved in the lake above a unit area of the seismites was mostly several times larger than that found in the seismite. The concentration of Ba^{2+} in DSB Ca-chloride brines is mostly lesser than that in the DSB Lake, ruling out the former as a source of Ba to the anomalies.

We propose that, during earthquakes, the uppermost bottom sediment layers in the DSB Lake were shaken and re-suspended into the overlying brine. The larger, faster-settling fragments and grains remained almost intact or were rapidly removed, unaffected, from the slurry. However, the finer grains remained in suspension for longer periods, allowing nucleation and growth of BM crystallites on their surfaces from the surrounding brine before reaching the bottom. The lag of Ba trapping behind the breccia accumulation and the asymmetrical peak shapes of the anomalies are accounted for by decreasing dilution of the Ba-rich finer particles by Ba-poor coarse grains during seismite accumulation, as reflected by the graded bedding of the seismite layers.

The supply rate of Ba^{2+} to the lake by freshwater and brines was more than sufficient to account for the buildup of Ba in recurring seismites separated by seismically quiescent intervals as short as 100 yr.

1. Introduction

The present paper is a first report of prominent barium concentration anomalies in seismically perturbed, brecciated layers within the Lisan Formation in the Dead Sea basin (DSB). The purpose of our study is two-fold:

1. Provision of geological and geochemical data pertinent to the occurrence and composition of the Ba-rich layers.
2. Evaluation of a possible relationship between the anomalies and frequent earthquakes that occurred during their formation.

1.1. Background

The Ba-enriched seismites are contained within the Pleistocene Lisan Formation exposed in the DSB (Fig. 1). The geology and hydrology of the basin, as well as the geochemistry of its waters and sediments have been thoroughly investigated during the last six decades (e.g. Bentor, 1961; Goldschmidt et al., 1967; Zak, 1967, 1997; Neev and Emery, 1967; Freund et al., 1970; Starinsky, 1974; Begin et al., 1974, 2004; Katz et al., 1977; Garfunkel, 1981; Stein et al., 1997, 2000; Stanislavsky and Gvirtzman, 1999; Moise et al., 2000; Krumgalz et al., 2000; Sagy et al., 2003; Klein-BenDavid et al., 2004, 2005; Kolodny et al., 2005; Bartov et al., 2006; Enzel et al., 2006; Torfstein, 2008; Katz and Starinsky, 2009; Torfstein et al., 2009).

* Corresponding author. Tel.: +972 2 658 4620; fax: +972 2 566 2581.
E-mail addresses: amitaia@vms.huji.ac.il (A. Katz), amotz@huji.ac.il (A. Agnon), shmulikm@tau.ac.il (S. Marco).
[1] Tel.: +972 2 658 4743; fax: +972 2 566 2581.
[2] Tel.: +972 3 640 7379; fax: +972 3 640 9282.

0012-821X/$ – see front matter © 2009 Elsevier B.V. All rights reserved.
doi:10.1016/j.epsl.2009.06.031

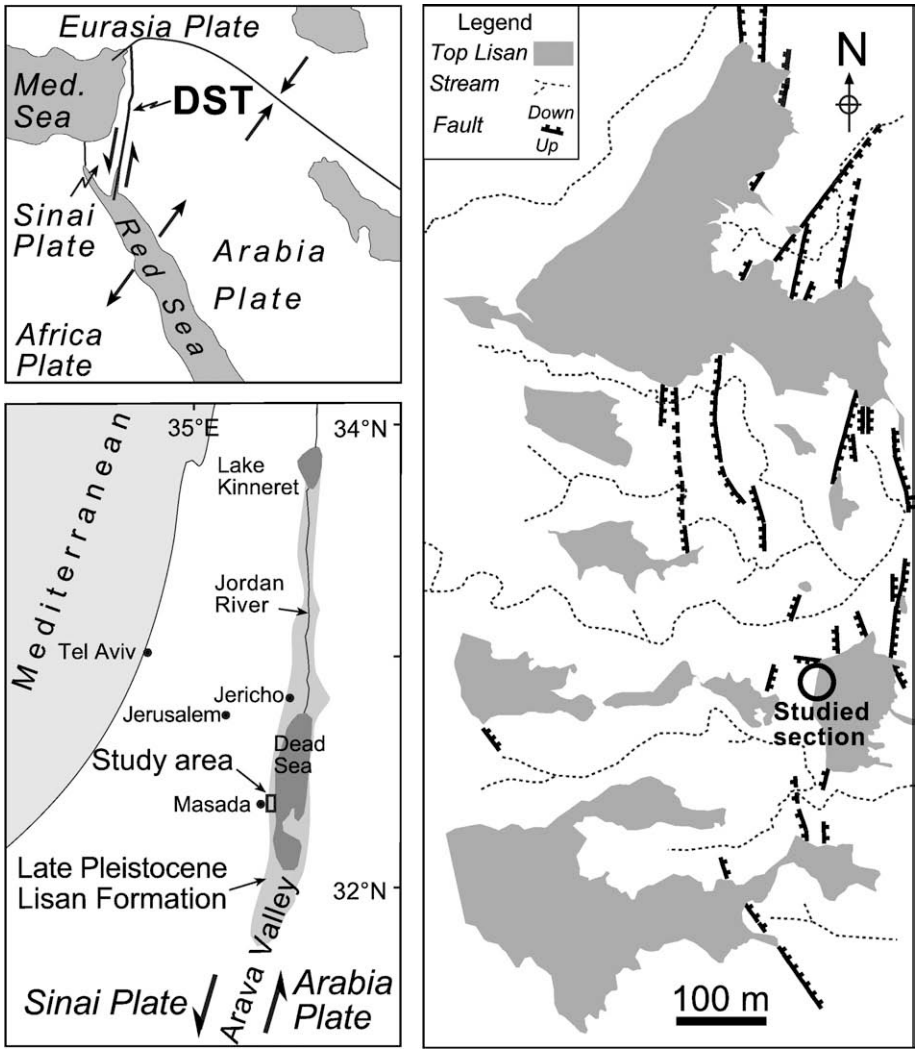

Fig. 1. Location map of the study area. Upper left: major plate boundaries in the Middle East and surroundings. DST = Dead Sea Transform. Lower left: The Dead Sea–Jordan–Arava Valley. The Lisan Fm. outcrops between Lake Kinneret (the Sea of Galilee) and the northern Arava Valley are highlighted in gray. Right: Detailed geological map of the study area.

1.2. The sediment record

Dead Sea basin sediments reflect two different environments of deposition that existed, sequentially, in the area since Neogene times. These are the Sedom marine evaporitic inland lagoon, and the lacustrine environment of the DSB Lake (Katz and Starinsky, 2009).

Recent studies shed light on the lacustrine sediment record deposited in the DSB Lake between ~720 and 70 ka (Waldmann et al., 2007; Torfstein et al., 2009; Katz and Starinsky, 2009). The overlying Lisan Formation (~70 ka to 14 ka, after Haase-Schramm et al., 2004) is up to ~40 m thick and is exposed between the northern Arava Valley in the south and Lake Kinneret (Sea of Galilee) in the north. The principal facies consists of alternating aragonite and detritus laminae ("AAD", after Marco, 1996), up to a few mm thick, where the former is perfectly preserved material which precipitated from the lake during summer, while the latter were washed into the lake during winters (Begin et al., 1974; Katz et al., 1977). The detritus consists of calcite, dolomite, quartz and clay. Laminated, massive and disseminated gypsum, and sandy beds make up the rest of the Lisan Fm. (Stein et al., 1997).

The Lisan Fm. is covered by the Zeelim Fm. deposited as of about 10.2 ka, containing similar detritus-evaporate laminated packages (Migowski et al., 2004, 2006).

1.3. The waters

Evidence supporting deposition of the Lisan sediments from a saline to hypersaline water body includes their fine, unperturbed lamination, the high water-soluble (chloride) salt content and the ion ratios therein, the predominance of aragonite laminae and Sr/Ca and Sr isotope ratios therein (Begin et al., 1974, 2004; Katz et al., 1977; Katz and Kolodny, 1989; Stein et al., 1997; Katz and Starinsky, 2009).

While practically all of the H_2O in DSB waters is of meteoric origin (Moise et al., 2000; Kolodny et al., 2005; Katz and Starinsky, 2009), the salts dissolved therein were inherited from ancient Mediterranean seawater and from upper Cretaceous carbonate rocks with which these waters interacted. The origin of the salts and later compositional modification are reflected by the Ca-chloridic nature ($Ca > (SO_4 + HCO_3)$) of the saline DSB waters. Starinsky (1974) proposed that the high salinity of the DSB brines was achieved by evaporation of seawater in the Sedom lagoon, from which they infiltrated into upper Cretaceous limestone aquifers. Most of the Mg in the brine was lost during dolomitization of the limestone, in exchange for Ca. The latter interacted with the brine's sulfate, precipitating gypsum and/or anhydrite. The low Na/Cl ratios in the brines resulted from halite crystallization in the original lagoon.

Please cite this article as: Katz, A., et al., Earthquake-induced barium anomalies in the Lisan Formation, Dead Sea Rift valley, Israel, Earth Planet. Sci. Lett. (2009), doi:10.1016/j.epsl.2009.06.031

No seawater incursions postdating the Sedom lagoon are known, leaving its chloride and accompanying marine solutes as the dominant source of salts in the DSB waters. Hydrological changes, Dead Sea transform tectonics and climatic fluctuations left their impact on the brines in the subsurface, as well as on the saline DSB Lake. A major feature of the DSB Lake was the intermittent stratification of its water column (Katz et al., 1977; Stein et al., 1997) brought about by the density difference between the feeding Ca-chloride brines ($\rho \leq 1.3$ g cm^{-3}) and freshwater runoff ($\rho \approx 1$ g cm^{-3}). Stratification of the lake must have occurred during lake level rises responding to "wetter" periods, when the freshwater input exceeded the evaporative loss of water. Katz and Starinsky (2009) showed that the characteristic AAD facies of the Lisan Fm. evolved during stratified periods of the lake. Independent observations demonstrating anoxic conditions that existed in the lake's deeper waters (Gavrieli et al., 2001; Torfstein et al., 2005, 2008) and the stratification of the modern Dead Sea that lasted well into the 20th century (Neev and Emery, 1967) support the same conclusion.

1.4. The Lisan seismites — the hosts of the Ba anomalies

The Lisan Formation, extending along a 220 km active plate boundary, provides an outstanding sediment sequence for paleoseismic studies (Seilacher, 1984; Marco and Agnon, 1995; Marco et al., 1996; Marco, 1996; Begin et al., 2005; Heifetz et al., 2005). It displays many well-preserved exposures and sensitive stratigraphic markers, as well as a continuous, densely-dated stratigraphic record (Schramm, 1997; Schramm et al., 2000; Haase-Schramm et al., 2004).

The Ba-anomalies occur within well-defined breccia layers, or seismites, contained within orderly-laminated sediment layers of the Lisan Fm. (Fig. 2). Field relations show that each seismite was formed by earthquake shaking (Marco and Agnon, 1995, 2005; Agnon et al., 2006). Such deformation structures were found also in younger (up to ≈10 ka) sediments around the Dead Sea (Enzel et al., 2000; Ken-Tor et al., 2001; Migowski et al., 2004). While all of the Ba anomalies found are confined to the Lisan seismites, similar seismites *without* Ba anomalies also appear in the studied area. An explanation of the first observation must be consistent also with the second.

Here we argue that the Ba anomalies were formed by stripping of Ba^{2+} ions from the DSB Lake water column, into Ba(Sr)SO_4 crystallites. The latter nucleated on the surfaces of grains suspended from the bottom into the lake by earthquake shaking, and during their settling and accumulation as seismites on the lake's bottom.

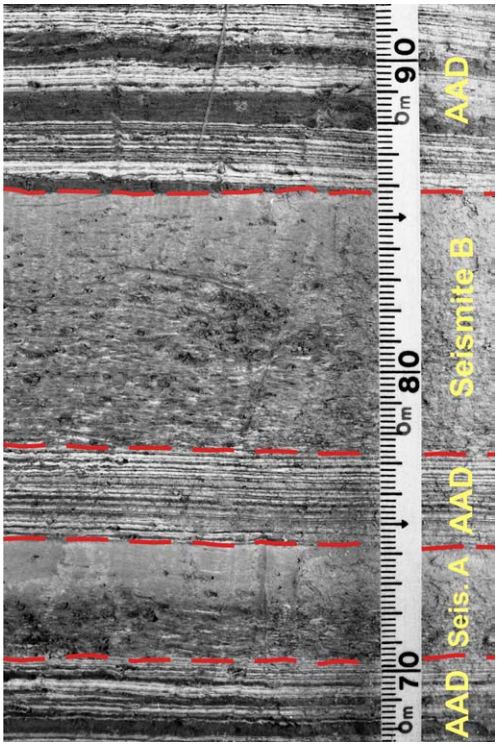

Fig. 2. A typical exposure of two seismites (A and B) in the Lisan Fm. near Masada. Both seismites display graded bedding. The vertical distance between the breccia layers is around 3 cm, equivalent to some 30 yr, as calculated from the sedimentation rate of about 1 mm yr^{-1} reported for this part of the section.

2. Methods

2.1. Field work

Sampling of the seismic breccias was carried out in the Lisan Fm. outcrops east of Masada (Fig. 1). Fresh 0.5–1.5 g samples were collected from vertical cliffs by manually pushing a 5 mm ID cylindrical steel corer into the soft, horizontal sediment layers. The vertical sampling profile included also a few centimeters of the undisturbed laminae beneath and above the seismite. Two larger samples ($\approx 30 \times 20 \times 20$ cm) from the Lisan Masada outcrop were carved from the outcrop to obtain better resolution than that provided by the corer. These samples served to study the detailed (mm scale) Ba distribution and behavior in pure aragonite and detritus laminae, as well as in the intervening seismite.

2.2. Laboratory work

2.2.1. Sample preparation

Water soluble salts were extracted by heating 0.1–0.5 g of the powdered sample in 25 ml H_2O in pressurized (120 psig) PFA Teflon® vessels at ≈115 (±10)°C within a CEM model MDS-2000 microwave system. The 40 min processing, included a gradual 10–12 min heat-up, followed by cooling down and depressurizing at room temperature. The supernatant solution was filtered (Whatman® #40 filter) into PMP volumetric flasks, diluted with deionized water (18.3 M-Ω cm^{-1}) and reserved for analysis.

The filtered solids were washed-back into the digestion vessel. Twenty ml dilute (1:10 v/v) HNO3 were added and the vessel was immediately sealed. Processing was carried on as with the water extraction. The extract solution was filtered into 100 ml PMP volumetric flasks and made up to volume with deionized water.

Separation of individual aragonite and detritus laminae followed Katz et al. (1977) procedure with slight modifications. Water and acid extraction was carried out as above.

2.2.2. Chemical analysis

Both the water and acid extracts were analyzed by ICP-OES using a fully automated Perkin-Elmer Optima-3000RL spectrometer with an internal precision of ±0.2–0.8% (1σ). Along with Ba we analyzed also Mg, Ca, Sr, Na, and SO_4. The following spectral lines were used: Na589.592, Mg280.270, Ca422.673, Sr407.771, S180.669, and Ba455.403.

2.2.3. Electron probe and SEM analysis

Selected samples were analyzed by electron microprobe (EMP) and high resolution scanning electron microscope (HR-SEM). EMP analysis was aimed at obtaining a semi quantitative chemical composition of the Ba mineral. The SEM analyses were found useful in revealing the micro-textural features of the BM and allowed to evaluate its crystallization environment and timing.

EMP analysis was carried out at the Hebrew University Institute of Earth Sciences on a JEOL JXA 8600 SUPERPROBE system. 10 nA beam current and 15 Kev accelerator voltages were used. The HR-SEM analyses were carried out at the Hebrew University Unit for Nano-

Please cite this article as: Katz, A., et al., Earthquake-induced barium anomalies in the Lisan Formation, Dead Sea Rift valley, Israel, Earth Planet. Sci. Lett. (2009), doi:10.1016/j.epsl.2009.06.031

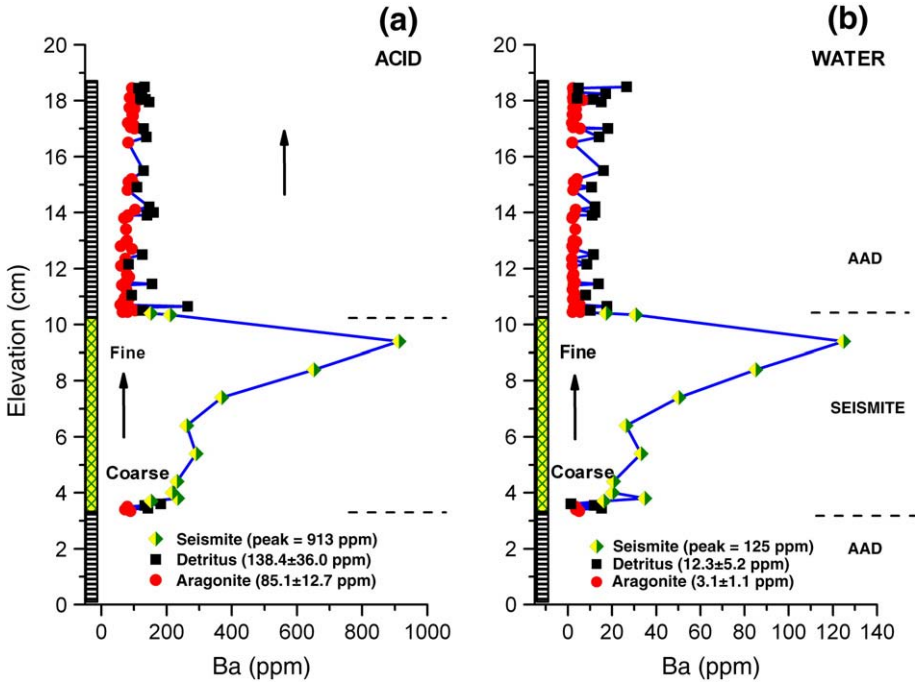

Fig. 3. The concentration of Ba in a vertical profile sampled through seismite "B" (Fig. 2). Acid dissolution of the samples (a) followed water extraction (b). Red filled circles represent aragonite laminae and black filled squares detritus laminae. Yellow/green rhombs mark seismites samples. Note the excellent sympathetic relationship between the curves in (a) and (b), supporting a common, intergranular Ba source for both solutions. (For interpretation of the references to color in this figure legend, the reader is referred to the web version of this article.)

characterization, using an FEI Sirion high resolution system operated at 10 kV accelerating voltage and equipped with Energy Dispersive X-Ray Spectroscopy (EDS of EDAX-TSL). The uncoated samples were mounted on standard aluminum stubs using double-sided conductive carbon tape. Morphological features and phase localization were observed under secondary (SE) and back-scattered (BSE) electron imaging at an analytical working distance of 5 mm.

3. Results and discussion

Chemical analyses of 90 samples collected from a vertical profile through seismite "B" (Fig. 2), are presented in Tables S1 (water extracts) and S2 (acid extracts of the water extracted samples). More aragonite than detritus laminae are listed in the tables because the latter are frequently too thin for separation. Characteristic Ba concentration and Ba/Ca ratio profiles across the seismite are displayed in Figs. 3 and 4. The slight difference in the seismite thickness between the exposure photo and the profile diagrams stems from the distance (ca. 20 m) between the sampled and the photographed sites (Fig. 2). For Ba, both its concentrations and ratios to Ca in the water extracts were calculated and displayed[3]. Acid dissolved Na, Sr and Mg concentration in profiles across the same seismite are presented for comparison in Fig. 5. HR-SEM images of the BM and the seismite matrix are given in Figs. 6–9 and S1. Electron microprobe analyses of selected BM crystallites are listed in Table 1.

3.1. Characterization of the Ba-anomalies and their host layers

Figs. 3 and 4 show that Ba in the seismite profile increases upwards, to values well above those in underlying or overlying detritus and aragonite laminae, before falling back towards its upper edge. At the same time, Na, Sr and Mg can readily be accounted for by mixing of aragonite and detritus layer fragments constituting the seismite (Fig. 5). Thus, the Ba profile suggests *addition*, rather than redistribution of local Ba, by the earthquake-triggered process.

Seismites display prominent graded bedding (Fig. 2), ranging from cm-scale fragments at their base to silt or even clay-sized particles at their top. The concentration of Ba in the lower (=coarser) part of a seismite is similar or slightly higher than that in the background laminae, increasing to the anomaly peak values only thereafter (Figs. 3 and 4)[4]. The anomalies are characteristically asymmetrical, sharply falling off at or slightly below the upper boundary. The absolute concentrations of Ba in the acid solutions are much higher than those of the water extracts of the same samples (Fig. 3a and b), yet allow an almost gap-free superposition of the two normalized graphs. The same holds true for the Ba/Ca acid — aqueous relationship (Fig. 4a and b). Both observations strongly support a common source of Ba for the water and acid sample solutions, and attribute the stated differences to the higher dissolution power of the acid rather than to different mineral phases. The water could dissolve Ba only from a mineral exposed to it while the acid would attack almost all protecting material (aragonite, calcite, and dolomite) and dissolve the Ba mineral anywhere. The behavior of Ba during sample dissolution is thus compatible with nucleation/growth on the matrix grains surface.

High resolution SEM textural analysis and back-scattered electron (BSE) images of seismite material containing the Ba-anomaly peak disclose μm-scale crystallites and aggregates of the BM, standing out in their brightness against the darker surrounding matrix grains and crystals (Figs. 6–9 and S1). Electron microprobe (EMP) analyses confirm that the crystallites are composed of $Ba(Sr)SO_4$ with Sr/Ba

[3] Calcium is a major component in the water and/or acid soluble fractions of detritus (calcite, dolomite, [gypsum]), evaporite (aragonite) and seismite (calcite, dolomite, aragonite and gypsum). Hence, normalization to Ca allows revealing contributions from other mineral sources (chlorides and silicates).

[4] The seismite material does not allow quantitative granulometric analysis. Dispersion of the *now*-dry breccias into water (or any other fluid required for that purpose) would result in their break down to individual grains and aggregates unrelated to their original size and shape. Neither would petrographic (thin section) examination be useful because of the very large size of many of the fragments and the clay size of the finer grains.

Please cite this article as: Katz, A., et al., Earthquake-induced barium anomalies in the Lisan Formation, Dead Sea Rift valley, Israel, Earth Planet. Sci. Lett. (2009), doi:10.1016/j.epsl.2009.06.031

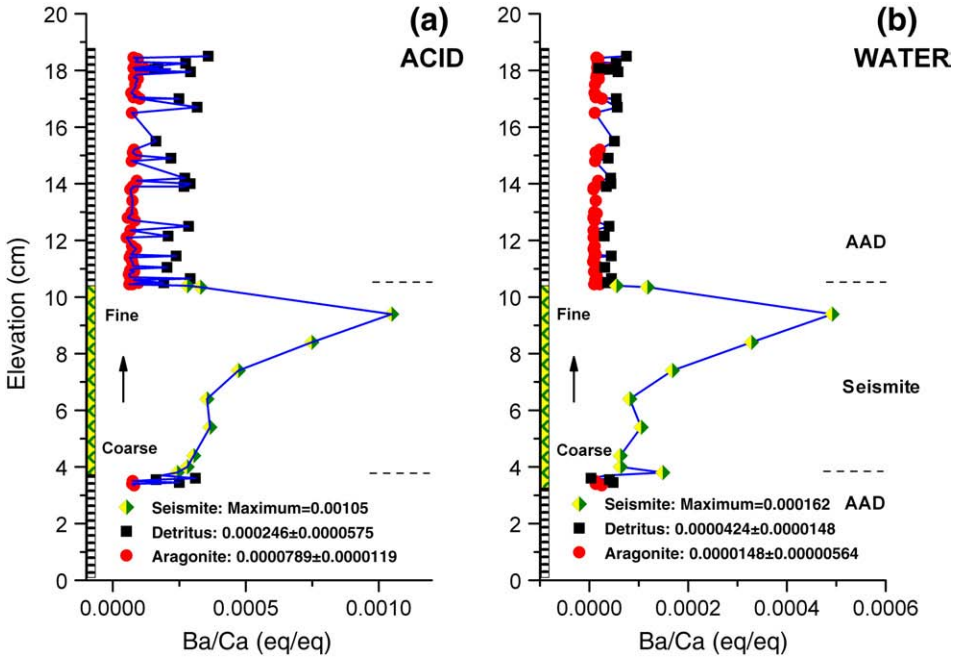

Fig. 4. Same as Fig. 3 after normalization of the data to Ca. The enrichment of Ba in the seismites is unrelated to that of Ca, which is the major ion comprising the bulk mineral composition of the seismites and of the normal (a-seismic) laminae (calcite, dolomite aragonite).

atom ratios averaging $0.295 \pm 0.103(1\sigma)$ (Table 1). Single homogeneous crystals of $(Ba,Sr)SO_4$ barite/celestite solid solutions, with Sr/Ba ratios around 0.2 have been synthesized long ago (Brower, 1973). However, only rarely were intermediate members of the $(Ba_{1-x}Sr_x)SO_4$ series with $0.1 < x < 0.9$ found in nature. Exact phase definition is beyond the scope of the present study.

3.2. The source of barium in the seismites

The source of Ba in the seismite anomalies may have been the overlying lake waters, interstitial bottom brines expelled back into the lake, or both. Derivation of Ba exclusively from the water column requires that its dissolved mass therein (per unit area) before the

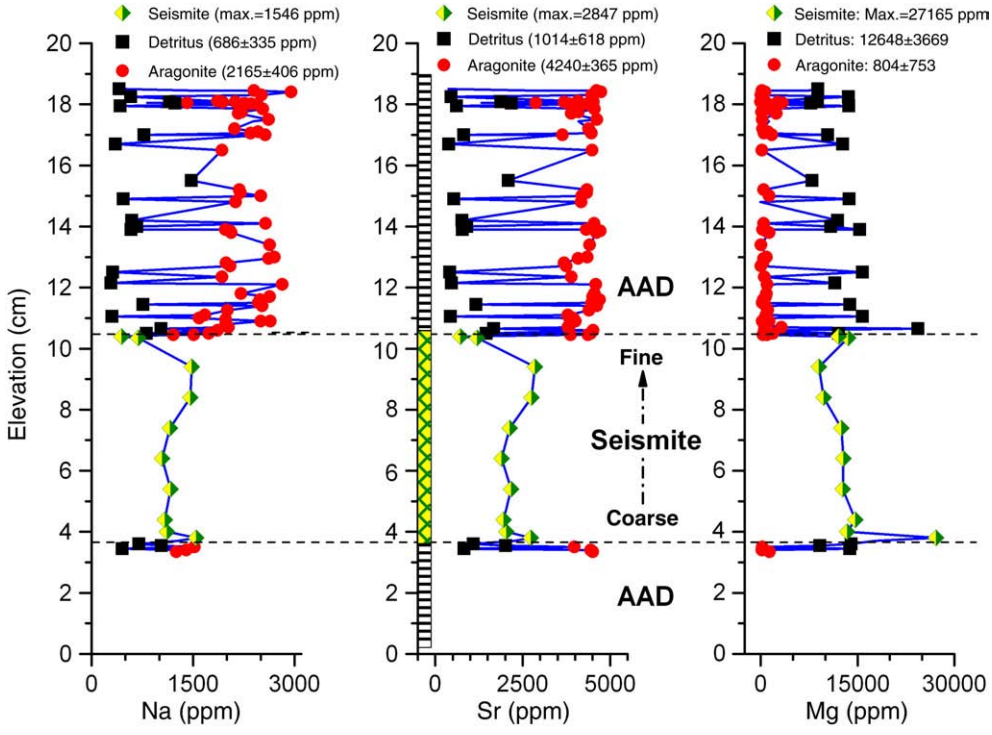

Fig. 5. Na, Sr and Mg concentration in the vertical profile through seismite "B". Only acid extract data is displayed (for water extract data please refer to Table S1). Unlike Ba, which is markedly enriched in the seismite, the concentrations of Na and Sr fall between their respective ones in pure aragonite and detritus laminae, resulting from mixing of detritus and aragonite fragments and grains. Moreover, in the seismite, the concentrations of both cations increase by 20–30% relative to their initial values in lower seismite zone, indicating the increase in the aragonite fraction in the finer grained upper zone. Mg displays, roughly, a mirror image of the Na and Sr behavior, reflecting the presence of dolomite in the detritus relative to the negligible concentration of this mineral in aragonite laminae.

Please cite this article as: Katz, A., et al., Earthquake-induced barium anomalies in the Lisan Formation, Dead Sea Rift valley, Israel, Earth Planet. Sci. Lett. (2009), doi:10.1016/j.epsl.2009.06.031

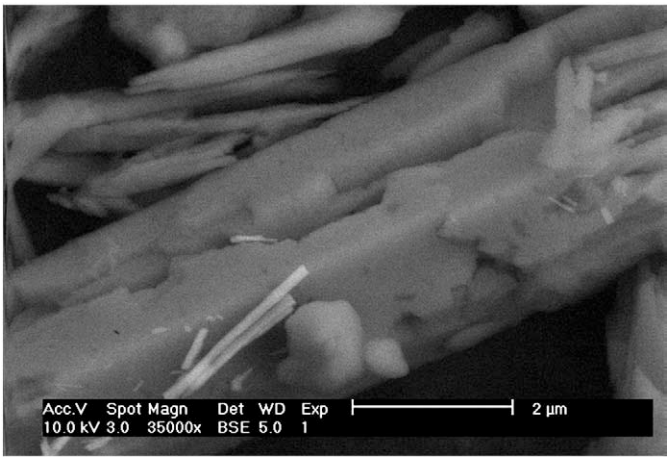

Fig. 6. BM crystallites (bright elongated prisms) that grew from a corroded surface of a much larger aragonite crystal grain. Note the few minute, barely visible dot-like BM crystallites left and above the three larger white prisms. These probably reflect incipient crystallization stages of the BM which was arrested when the aragonite carrier raft became grounded in the accumulating seismite.

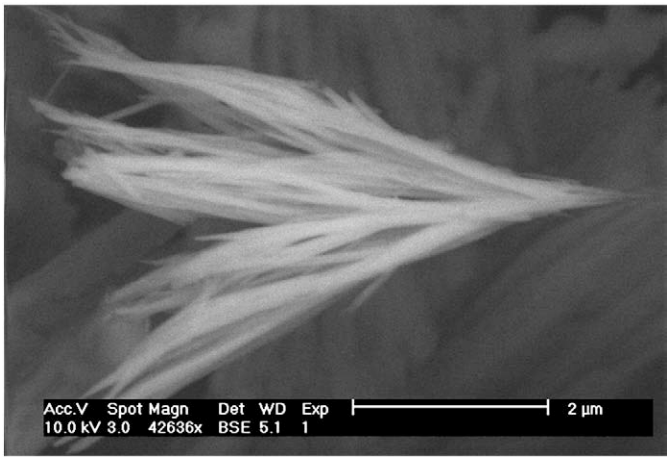

Fig. 7. A branching, dendritic aggregate of BM crystallites. The individual crystal prisms are extremely thin and delicate accounting for their "curved" appearance.

earthquake exceeded that in the seismite. Considering feasible chemical yields and (albeit low) solubility of relevant Ba minerals this is a *minimum* prerequisite. A crude mass balance test of this question follows below. A negative result (i.e. $Ba_{water}<Ba_{seismite}$) would rule out a singular water column source while a positive one would support, but not necessarily prove, the contrary.

3.2.1. Water column — breccia mass balance for barium

A mass balance between the Ba in the seismites and that in the overlying water heavily leans on a reliable estimate of the concentration of Ba^{2+} in the DSB Lake. Thermodynamic, Pitzer-type modeling, developed by Krumgalz et al. (2000, 2002) for calculating mineral solubility in modern Dead Sea water reveals significant supersaturation with respect to barite. Moreover, chemical analyses of Dead Sea waters evaporated to various degrees (Zilberman-Kron, 2008) indicate increasingly higher Ω_{barite} values[5] upon higher salinity. Hence, although barite is abundant in the Dead Sea rift valley sediments and rocks its calculated solubility may not represent the actual Ba^{2+} concentration that prevailed in the ancient brine.

A large number of chemical analyses relevant to the Ba^{2+} mass balance have accumulated during the years (Beyth, 1977; Katz and Ganor, 1985; Ganor, 1986; Chan and Chung, 1987; Ganor and Katz, 1989; Moise et al., 2000; Zilberman-Kron, 2008; Katz and Starinsky, 2009).

Experimental evaporation of Dead Sea water in the field (Zilberman-Kron, 2008) shows Ba^{2+} to remain conservative up to a 4-fold concentration ($I\approx 21$). The same conclusion can be reached from the behavior of Ba^{2+} in halite evaporation ponds of the potash industry in the DSB (Ganor, 1986), where Dead Sea water evaporates up to a 2-fold concentration. Conservative behavior of Ba^{2+} was also noted in Dead Sea water upon its dilution to various degrees by brackish springs in large (hundreds of meters across) natural pools. The Ba^{2+} in the diluted mixtures displays linear concentration relationships with other conservative solutes such as Ca, Sr and Li (Zilberman-Kron, 2008). Hence, it can be concluded that the concentration of Ba^{2+} in the DSB Ca-chloride brines is not controlled by the solubility of $BaSO_4$ but is kinetically retarded, at least up to a 4-fold concentration of modern Dead Sea water. If so, the Ba^{2+} concentration in the lake can be roughly estimated by division of its concentration in the Dead Sea by the ratio between the ancient DSB Lake volume preceding the earthquake and that of the modern Dead Sea (V_{DSB}/V_{DS}). This type of calculations can be expected to yield reasonable results for well mixed lakes, but is insensitive to stratification of the water column, a frequent situation during the DSB Lake history. Upon such circumstances, the freshwater inflow mixes only with the upper water layer of the lake, forming a diluted, upper water mass, above the deeper, unchanged brine. Application of dilution factors to a stratified lake would result in some underestimation of the Ba^{2+} concentration in the lower water mass and in too high concentrations in the overlying waters. Because the accurate depth of the halocline that separated the two water masses during the period of interest is unknown, refinement of the calculation is not possible. Yet, if the seismite Ba excess was derived from the water column, then the lower water mass must have played a more dominant role in the process than the upper waters of the lake. We will therefore attempt to estimate the mass of Ba^{2+} available to the breccias from the water column, assuming that the lake was homogeneous before its last level rise, neglecting contribution of barium from the fresher upper layer.

3.2.1.1. Estimation of the Ba mass in the water column. The position of the seismites under study in the Lisan Fm. roughly corresponds to a

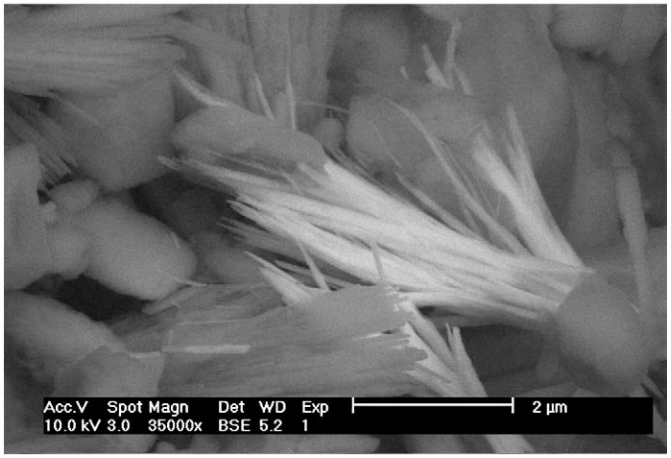

Fig. 8. Similar to Fig. 7, however clearly displaying the very large difference between the size of the BM crystals and the much larger matrix grains on which they crystallized.

[5] Ω designates the degree of saturation of the solution with respect to the subscripted mineral, and is defined as IAP/K_{sp} where IAP is the ion activity product of the respective ions in solution and K_{sp} stands for the solubility product of the mineral under regard. For a saturated solution at equilibrium $\Omega=1$.

Please cite this article as: Katz, A., et al., Earthquake-induced barium anomalies in the Lisan Formation, Dead Sea Rift valley, Israel, Earth Planet. Sci. Lett. (2009), doi:10.1016/j.epsl.2009.06.031

27–17 ka old sediment section (after Haase-Schramm et al., 2004; Prasad et al., 2004), during which the lake's level rose from about 270 mbsl to 165 mbsl (Bartov et al., 2002, 2006). These levels correspond to lake volumes of ≈300 and ≈600 km^3, respectively (calculated from Hall's (1996) diagram). At the level of 270 mbsl, the dilution factor of the lake with respect to the modern Dead Sea (level ~420 mbsl; volume ~120 km^3) would be around 300/120 = 2.5. The 165 mbsl level would correspond to a dilution of 600/120 = 5. The concentration of Ba^{2+} in the Dead Sea amounts to 4.86 mg L^{-1} at a brine density $\rho = 1.2357$ g cm^{-3} (Zilberman-Kron, 2008). Division of this value (4.86 mg L^{-1}) by the calculated dilution factors (~2.5 and ~5) yields the concentration range of Ba^{2+} in the (non-stratified) lake during the seismite deposition, namely 1–2 mg L^{-1}.

3.2.1.2. Estimation of the Ba mass in the seismite. The thickness of seismite layers and Ba-anomalies in the Lisan Formation considerably varies from place to place. Here we relate to a seismite of a 10 cm "nominal" thickness that includes a Ba anomaly peaking, symmetrically, to 1000 ppm ($C_{Ba,An}$) above a ~100 ppm normal background ($C_{Ba,BG}$). Also, we assume a length of 5 cm to the baseline under the peak and a bulk density, $\rho = 2$ g cm^{-3} to the seismite material. Approximating the anomaly's cross section by an isosceles triangle with a 5 cm base (a) and (1000–100) = 900 ppm height (h), the mass of Ba (M_{Ba}) per unit area ($s = 1$ cm^2) of the seismite contained therein is given by

$$M_{Ba} = \frac{1}{2}(a \cdot s \cdot h \cdot \rho) = \frac{1}{2}(5 \cdot 1 \cdot 900 \cdot 2) = 4.5 \text{mg Ba cm}^{-2}. \quad (1)$$

Recalling the concentration range of Ba^{2+} in the water column estimated above (1–2 mg L^{-1}), the trapped Ba can be provided by stripping, at a 100% yield, a water column anywhere between 45 and 22.5 m long.

The DSB Lake level during the relevant period was much higher than that of the modern Dead Sea (~420 mbsl) implying also greater water depth, well exceeding the 22.5–45 m length of the water column Ba reservoir required above.

3.2.1.3. Local effects on the Ba balance. Two causes, both of local and lesser significance, may have affected the Ba balance.

1. Ba supply to shallow environments along the lake's margins may have been restricted due to insufficient depth of the overlying water column. This effect could furthermore be amplified by a stratified lake situation where Ba^{2+} in the relatively diluted upper water layer must have been depleted.
2. Lateral mixing of brine between the seismically perturbed lake zone and adjacent waters overlying quiescent bottom would promote the import of Ba^{2+} into the water column above the seismite.

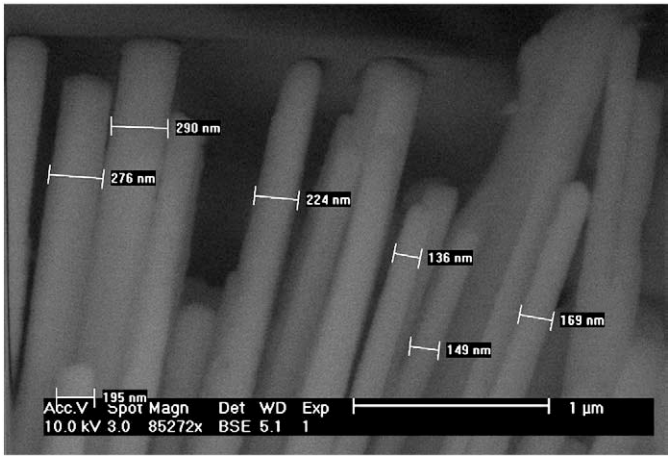

Fig. 9. A group of sub parallel BM crystallites belonging to a dendritic aggregate, showing typical 100–300 nm width of their prisms. The crystals grew on a highly irregular surface of a calcite grain (not shown) and stopped their growth upon hitting the opposite side of the irregular void.

Table 1
Electron microprobe (EMP) analyses of BM crystallites from a seismite in the Masada section of the Lisan Formation.

Sample		Mg	Ca	Sr	Ba	S
1121A	Atom %	0.28	3.60	1.42	15.08	12.07
	wt.%	0.11	2.38	2.06	34.22	6.39
1121B	Atom %	1.11	3.26	2.90	8.33	10.77
	wt.%	0.79	3.83	7.45	33.56	10.13
1121C	Atom %	1.19	2.87	3.50	10.08	13.28
	wt.%	0.82	3.26	8.70	39.27	12.07
1122A	Atom %	1.08	11.52	2.50	6.70	8.23
	wt.%	0.60	10.56	5.01	21.07	6.04
1122B	Atom %	0.34	11.38	2.27	11.69	10.15
	wt.%	0.12	6.82	2.97	24.01	4.87
1122E	Atom %	0.97	6.14	3.38	7.51	10.59
	wt.%	0.64	6.74	8.12	28.25	9.30
1123A	Atom %	0.81	12.61	1.46	5.76	6.15
	wt.%	0.38	9.83	2.48	15.38	3.83
1123C	Atom %	1.19	15.57	2.16	7.33	6.03
	wt.%	0.57	12.26	3.72	19.78	3.80
1124A	Atom %	2.11	10.75	1.42	5.95	6.56
	wt.%	1.48	12.40	3.57	23.52	6.05
1124B	Atom %	0.72	4.69	2.93	8.21	10.24
	wt.%	0.50	5.35	7.31	32.10	9.34

Both the weight and atom percentages are given.

3.2.2. External Ba sources

The potential of the DSB Lake as a Ba source to the seismites by itself does not exclude contributions from external sources such as saline subsurface fluids (Starinsky, 1974; Katz and Starinsky, 2009). Many of these are characterized by their H_2S odor, relating the respective brine to bacterial sulfate reduction (BSR) in the bottom waters of the episodically anoxic lake. BSR would facilitate increase in Ba^{+2} concentration, which may be maintained in the isolated subsurface aquifers. Evidence of earthquake-related groundwater injection, and models explaining this association, have been reported in recent literature. Most reported cases refer to post-seismic effects, but various mechanical models of earthquake generation are compatible with precursory effects as well (Muir-Wood and King, 1993).

Relevant to the question are sudden and prolonged increases in the discharge of springs located some 200 km north of the epicenter of the Nuweiba October 22, 1995 Mw 7.2 earthquake reported by Yechieli and Bein (2002). The same event was also marked by a change in chemical composition of the springs, well within the Dead Sea rift valley, shortly after the earthquake (L. Enmar, pers. commun.). However, chemical analyses reported by Moise et al. (2000) and by Zilberman-Kron (2008) do not support direct injection of subsurface brines as a source for the Ba in the seismites. Saline Ca-chloride, H_2S-laden waters discharging from springs, seepages and wells along the western shores of the Dead Sea do not show Ba^{2+} enrichment relative to surface waters of similar salinity.

3.2.3. The timing and duration of Ba trapping

The following observations guide us to the timing and duration of the Ba removal from the water column into the seismites:

1. The finely laminated Lisan sediments are extremely impermeable to water, as shown by the excellent preservation of their original aragonite (Katz et al., 1977) and water soluble salts (Katz and Kolodny, 1989).

Please cite this article as: Katz, A., et al., Earthquake-induced barium anomalies in the Lisan Formation, Dead Sea Rift valley, Israel, Earth Planet. Sci. Lett. (2009), doi:10.1016/j.epsl.2009.06.031

2. None of the Ba anomalies studied extends beyond the top of host seismite.
3. The lift-off point of Ba concentration from background values mostly appears well above the base of the seismite (Figs. 3 and 4). Significant in this regard is the apparent coincidence of the normal background zone of the lower part of the anomaly with the lower, coarsely fragmented part of the breccias (Fig. 2).
4. No horizontal, continuous and undistorted aragonite laminae have been found within the seismites (Fig. 2). Rather, only discontinuous, perturbed aragonite or detritus laminae, which are deformed, torn apart fragments of laminated AAD material, were found. Hence, accumulation of the seismites, following the onset of the relevant earthquakes, must have been completed *before* the deposition of the first normal (i.e. post-seismic) aragonite lamina. An aragonite lamina represents a period of up to a few years (Katz and Starinsky, 2009). If the accumulation period of the seismite would have taken longer, one would expect one or more aragonite-detritus pair to appear therein, which is not the case. The detritus laminae, interlayered between the aragonite ones, represent winter floods into the DSB Lake (Begin et al., 1974; Machlus et al., 2000) and therefore must have been deposited during an even shorter (~seasonal) time.

Consequently, post depositional introduction of Ba into the seismite is unlikely (#1) and we conclude that Ba emplacement terminated before resumption of normal sedimentation after the seismite deposition (#2). Excluding diagenesis, observation #3 indicates that Ba supply to the seismites was attenuated, or that its trapping process was less efficient during the initial accumulation phase than later. The absence of continuous aragonite or detritus laminae *within* seismites (#4) constrains the length of the deposition period of a seismite and, along with it, the duration of Ba trapping to a few years at most (#5).

3.2.4. The Ba trapping mechanism and its consequences

The following points summarize the main observations relevant to the trapping of Ba in the seismites:

1. The BM crystallites started their growth on solid surfaces of their adjacent matrix grains, to which they are still anchored (Figs. 6 and 8). No free-floating (i.e. unattached) BM crystallites have been found in the seismites.
2. In contrast to the seismites, which show prominent graded bedding, the size of the BM crystallites and their aggregates shows no consistent relation to their position in the profile, or to the size of the carrier grains (Figs. 6 and 8).
3. The size of individual crystallites and aggregates of the BM is always much smaller than that of the seismite matrix grains (let alone fragments), frequently differing by a few orders of magnitude (Fig. 6).
4. Extremely fine crystallization textures are displayed by the BM, including wavy or radiating, fibrous or prismatic-lamellar crystallites and aggregates (Figs. 6–9).
5. As far as the BM crystallites are concerned, the only difference between the peak zone of a Ba anomaly and its flanks is the distinctly denser population of the BM crystals within the peak zone.
6. The Sr/Ba ratios in the BM crystals show a rather wide variation (0.1–0.45; average = $0.295 \pm 0.103(1\sigma)$; data from Table 1).

Based on the above observations we propose that the Ba was stripped from the lake water by sediment particles that were re-suspended into the overlying brine by earthquake shaking. These provided the rafts needed for the BM nucleation and growth (#1). Both nucleation density and subsequent growth of the BM crystallites must have been dependent on the residence time of the suspended sediment grains in the water, which in turn was dictated by their size. Large fragments and particles would rapidly settle down and accumulate as a graded breccia bed on the bottom (#2), leaving little time for nucleation and growth in the water column. Moreover, not only had the larger fragments a shorter, post-seismic residence time in the brine but they could not have been suspended as far up in the water column as could the smaller grains. Thus, a small particle was exposed to a longer settling path allowing it to scavenge more Ba. No wonder then that no hydrodynamic relation is revealed between the seismite matrix carrier grains and the BM crystallites attached to them (#3). The same reasoning may explain the behavior of Ba during the early deposition phase of the seismites. The corresponding, lower part of the graded breccia is its coarsest, consisting of cm-scale fragments which, albeit deformed and torn apart, remained almost intact during the earthquake shaking. If so, their Ba concentration should reflect the unchanged background values of the unperturbed Lisan sediments, as they indeed do.

The difference in population density of the BM between the anomaly peak zone and its flank are readily accountable along the same lines. The crystallite population density is a function of their nucleation rate ($N\,s^{-1}\,cm^{-3}$)[6] on the settling grains which, under otherwise similar conditions, is dependent on available surface area of the substrate grain. The smaller the grain size of a given sediment mass, the larger becomes its surface area, as evidenced by the location of the anomaly peak close to the upper boundary of the finest grained zone of the seismite.

The peak shapes of the anomalies are frequently asymmetric. The moderate (lower) flank reflects the gradually diminishing dilution of the fine (BM-rich) particles of the breccia by the coarser (BM-poor) grains and fragments. The steep Ba concentration decline above the anomaly's maximum may reflect the consumption of suitable BM-carrier grains from the water column. It is likely that nucleation rate is not only restricted by the available surface area of the fine particles, but also by their mineral composition and surface characteristics. Hence, some accumulation of the seismite material may have proceeded *without* significant addition of BM crystallites to the seismite.

The wide variation of the Sr/Ba ratio in the BM (#6) needs some further elaboration. The fraction of Sr^{2+} scavenged from the water column into the settling BM crystals must have been negligible in comparison to its total mass there. (DSB brines typically contain a few hundred mg Sr L^{-1}). Hence, Sr trapping in the seismites should not bring about a measurable change in its concentration in the lake. This is not the case with Ba^{2+} though, whose concentration in the water column is estimated to be within 1–2 mg L^{-1} (Section 3.2.1.1). Although mostly $Ba_{water} \gg Ba_{scavenged}$, removal of a few to several percent of the Ba^{2+} from the water during the deposition of the material hosting the Ba peak may result in a heterogeneous concentration of this ion in solution, reflected in the variable Sr/Ba ratio in the crystallites.

3.2.5. Ba replenishment upon earthquake recurrence

High resolution stratigraphic studies of the outcrops relevant to our study were carried out by Marco and Agnon (2005) and by Agnon et al. (2006). These revealed repeated earthquake-faulting on the same planes, accompanied by seismite formation, for limited periods on the order of a few thousands of years. Locally, each fault exhibits a cluster of 3–5 slip events bracketing a period up to 4 kyr long with greatly varying time gaps between slips within a given cluster. Coalescence of clusters from individual faults leads to clustering periods of ~10 kyr with quiescent periods of comparable duration.

[6] Expressed as N = Number of nuclei per unit time (s) per unit volume (cm^3) of the seismite.

Please cite this article as: Katz, A., et al., Earthquake-induced barium anomalies in the Lisan Formation, Dead Sea Rift valley, Israel, Earth Planet. Sci. Lett. (2009), doi:10.1016/j.epsl.2009.06.031

Removal of dissolved Ba^{2+} from the DSB Lake into these seismites was thus repetitive and, on a time scale of hundreds to thousands of years, quite frequent. This raises the question whether, under otherwise similar conditions, the Ba^{2+} re-supply rate into the lake constrained the magnitude of the Ba anomalies in successive seismites. If replenishment rate of Ba^{2+} to the lake was smaller than its scavenging rate due to trapping in seismites, consecutive anomalies would display decreasing concentration peaks in time. If the Ba^{2+} supply rate was similar or larger than its intake rate into the breccias, a quasi steady state would develop, reflected by Ba concentration peaks of similar magnitude within seismites of similar pre-seismic history. Under the latter scenario one would also expect a generally sympathetic relationship between the length of the a-seismic time gap and peak magnitude in seismites. Moreover, because mixing time in such lakes was very likely much shorter than earthquake recurrence time, normalization of anomaly magnitude to the relevant recurrence time for a given seismite may allow identification of an earthquake that escaped recording in the same section. While systematic sampling and analysis of seismites that is required for resolving the issue under regard still waits ahead, examination of the available data already at hand allows deriving some helpful ideas for future work:

1. Fig. 2 displays a succession of two seismites, A and B, separated by ~3 cm of normally laminated Lisan sediment. The Ba anomaly in B is plotted in Figs. 3 and 4. Technical problems prevented obtaining data of similar resolution and precision for seismite A, yet from what we have it is clear that the excess Ba mass in B is about twice of that concealed in A.
2. The time elapsed between the earthquakes that gave birth to seismites A and B can be deduced from the combined thickness of the non seismic sediment package separating them (~3 cm) and that of B (~8 cm), totaling ~11 cm. Using a nominal sedimentation rate of ~1 mm/yr (Hasse-Schramm et al., 2004) for the Lisan section under regard, the time equivalent looked for is slightly over 100 yr.
3. The extra mass of Ba concealed in seismite B can be roughly estimated using Eq. (1). Thus, letting $a \sim 5$ cm, $s = 1$ cm^2, $h \sim (913–150) \sim 760$ ppm[7], and $\rho = 2$ g cm^{-3},

$$M_{Ba,B} = \frac{1}{2}(a \cdot s \cdot h \cdot \rho) = \frac{1}{2}(5 \cdot 1 \cdot 760 \cdot 2) = 3.8\,\text{mg Ba cm}^{-2}. \quad (2)$$

Similarly, $M_{Ba,A}$ would amount to $M_{Ba,B}/2 = 1.9$ mg Ba cm^{-2}. To compensate for the Ba^{2+} loss from the water column into seismite A before the onset of earthquake B an influx of ~1900/100 = 19 μg Ba cm^{-2} yr^{-1} must be maintained. Dissolved Ba^{2+} enters the DSB Lake both via freshwater runoff and from saline springs discharge. The concentrations of Ba^{2+} in modern freshwater sources varies anywhere between 50 and 200 μg L^{-1} (Moise et al., 2000; Katz, unpublished data). The saline springs that were proposed by Starinsky (1974) to represent the ancient brines discharging into the DSB Lake hold ~1.5 mg Ba L^{-1} at TDS = 191 g L^{-1} (Zilberman-Kron, 2008, sample #33, En Kedem spring). The average fluxes of fresh and saline water into the DSB Lake can be calculated deploying the Ca–Mg mass balance equations developed by Katz and Starinsky (2009), yielding 0.28 and 0.0007 L cm^{-2} yr^{-1}, respectively. Hence, the annual import of Ba^{2+} by freshwater is between $0.28 \cdot 50 = 14$ and $0.28 \cdot 200 = 56$ μg Ba cm^{-2}, whereas saline waters contribute only a negligible addition of $0.0007 \cdot 1500 = 1$ μg Ba cm^{-2} yr^{-1} to the budget. Depending on the concentration of Ba^{2+} assigned to freshwater, the flux of this cation into the DSB Lake has been anywhere in the range of 15–60 μg cm^{-2} yr^{-1}, more than is needed for compensating the Ba uptake in seismite A.

Despite the uncertainties inherent in the above balance, it seems that the supply rate of Ba to the DSB Lake set no constraint on the Ba concentrations in seismites, even under an earthquake recurrence rate of 100 yr. Actually, if the maximum supersaturation tolerable by the lake with respect to $BaSO_4$ was higher than that calculated for the modern Dead Sea, than even larger Ba masses could accumulate in the water column during seismically quiescent periods. This is significant in view of the long existence (>650 kyr) of the DSB Lake before the deposition of the Lisan Formation (Torfstein et al., 2009).

3.2.6. Anomaly-free breccia layers

Seismites free of Ba anomalies do occur in the Lisan Fm. but, according to our preliminary survey, are not common. Three different reasons, emerging from our study, may also account for their occasional absence:

a) Insufficient suspension of fine sediment during the earthquake.
b) Insufficient water depth at the site affected by the earthquake.
c) Lake stratification.

While the three causes listed above are independent of each other, (b) and (c) led to the same result.

Insufficient fined material suspended from the bottom sediments by the earthquake (#a) would fail to produce the needed amount of suitable scavenging material.

Too shallow waters above the seismically perturbed lake bottom (#b) will not hold sufficient Ba^{2+} for scavenging, resulting in low amplitude anomalies, if any.

Lake stratification (#c) is expected to decrease the effective thickness of the (Ba-rich) lower water layer, along with the mass of dissolved Ba^{2+} available for stripping, resulting in anomalies similar to those caused by (#b).

3.2.7. Ba^{2+} scavenging during normal (a-seismic) sedimentation

The Ba anomalies are attributed here to scavenging of Ba^2 by settling particles, suspended from the lake bottom by earthquake shaking. This raises the question why a similar process did not occur during winter floods, which imported into the lake their detritus, or during high summer, when aragonite crystals forming in the upper waters rained out of the lake. At this stage we can add little more than suggesting that these observations may be related to differences in mineral composition of the particles that settled through the water column during seismically-active and quiescent periods.

The Lisan section under study displays a clear-cut separation between aragonite and detritus laminae (Fig. 2). The well defined separation has been attributed to the non-overlapping deposition periods of the materials involved. Aragonite is a primary precipitate from the upper water column resulting from the interaction of the dissolved Ca^{2+} and HCO_3^- imported during winter by freshwater[8]. Crystallization of this mineral is arrested until summer, when its precipitation is enforced by seasonal heating and as a consequence of evaporation. The delay in aragonite precipitation enables the lake to get rid of the suspended detritus before the onset of aragonite precipitation in summer. The water column can therefore be visualized as an aqueous medium through which fluxes of detrital particles (calcite, dolomite, with minor quartz, clay and organic debris) settle to the bottom during winter, followed by a pause in sedimentation during spring and early summer, and by aragonite precipitation somewhat later. The higher purity of aragonite laminae with respect to detritus content, than that of the detritus laminae relative to aragonite, is accounted for by stir up of bottom sediment by waves during winter storms, which are rarer and weaker during high

[7] A background of 150 ppm Ba is assumed to compensate for the background slope and for its slightly elevated lower part.

[8] Because in the freshwater $HCO_3^- > Ca^{2+}$ (in equivalent units), the balance is made up by Ca^{2+} from the lake's Ca-chloride brine (see discussions in Katz et al., 1977; Stein et al., 1997; Katz and Starinsky, 2009).

Please cite this article as: Katz, A., et al., Earthquake-induced barium anomalies in the Lisan Formation, Dead Sea Rift valley, Israel, Earth Planet. Sci. Lett. (2009), doi:10.1016/j.epsl.2009.06.031

summer. In contrast to the calcite, dolomite quartz and clay minerals, no gypsum particles could be washed into the lake by fresh flood water, which was strongly undersaturated with respect to $CaSO_4$. The few laminae and massive beds of gypsum found in the Lisan Fm. reflect relatively rare precipitation events induced by discrete episodes of lake level decline (Stein et al., 1997; Torfstein et al., 2008). Diagenetic, *insitu* crystallization of gypsum is evidenced by the presence of flat, radiating aggregates of this mineral "sandwiched" between, and parallel, to the AAD laminae.

Sediment suspension by earthquake shaking, unlike seasonally alternating normal particle settling, would not discriminate between aragonite and the various minerals comprising the detritus laminae and gypsum. The resulting multi-mineral slurry produced by an earthquake must therefore be very different in this regard from the lake waters during seismically quiescent periods. One or more diagenetically-formed minerals in this slurry, which has not yet been disclosed by our HR-SEM analyses, may have provided a preferred nucleation substrate for the BM, accounting for the localization of the Ba anomalies in seismites rather than in normal AAD laminated layers. Of all minerals mentioned above, gypsum should be favored as a promising candidate. Shaking of a massive bottom sediment parcel by an earthquake would very likely release some of its gypsum content into the water. Readily available sulfate on the surface of this mineral would obviously not interfere with nucleation of a $BaSO_4$ mineral.

4. Summary and conclusions

Seismites, in the form of breccia layers in the Lisan Fm. along the Dead Sea western shore display conspicuous Ba concentration anomalies, well above background values measured in underlying and overlying sediments. Ba concentrations in the seismites gradually increase upwards, attaining maxima close to, or at the upper boundary of the breccias. HR-SEM and EMP analyses show that the excess Ba resides within micron-scale, $Ba(Sr)SO_4$ crystallites anchored to the matrix grains.

The following evidence and considerations show that the Ba in the seismites was scavenged from the water column of the DSB Lake by sediment particles suspended into the lake by seismic shaking:

1. The Ba anomalies are restricted to the seismites.
2. The mass of Ba in the anomalous zones significantly exceeds that which is contained in underlying and overlying sediment packages of equal thickness, indicating that the Ba within an anomaly represents a net *addition*, and not redistribution of normal, unperturbed sediment Ba.
3. The Ba in the seismite material resides in minute (~1 μm) $Ba(Sr)SO_4$ mineral crystallites and in their minuscule aggregates. These display a characteristic growth patterns from the surfaces of much larger matrix grains of the host breccias.
4. The size of the Ba mineral crystals is unrelated to that of the surrounding grains and fragments, or to the (time related) vertical position of the mineral in the seismite profile, in sharp contrast to the marked graded sorting of the matrix grains and fragments in the host-seismite.
5. The concentration gradients that characterize the anomalies reflect the change in the number of crystallites per unit volume of the seismite, not their size.
6. The nucleation and growth of the Ba mineral on the seismite grains started and ended during the accumulation of the seismite layer, which lasted a few years at most.
7. The absence of Ba anomalies in some seismites is a result of a local insufficiency in dissolved Ba^{2+} in the overlying water column, which would occur in near-shore shallow environments. Similarly, lake stratification would result in a decrease in the concentration of Ba in the upper waters and a decrease in the total mass of Ba available for trapping. Another reason leading to anomaly-free seismites may be insufficient sediment shaking (and consequent dispersion) by the earthquake.
8. The vertical position and shape of Ba anomalies in seismites are dictated by the dilution ratio of the Ba-rich finer grained particles by coarse, Ba-poor fragments that remained almost intact during the earthquake.
9. The magnitude of the Ba anomalies is not limited by the recurrence rate of earthquakes at least up to a 0.01 yr^{-1} frequency, because the flux of Ba^{2+} into the lake readily compensates for its loss in the seismites.

Acknowledgements

We are grateful to Dr. Elad Israeli, Mrs. Tamar Shalev, and Dr. Inna Popov from the Hebrew University for their professional assistance in SEM and EMP analysis. Mrs. Ahuva Agranat and Enat Kasher carried out the elaborate water and acid extractions and analytical preparations in the Hebrew University geochemical laboratory. Ofra Klein-BenDavid was very helpful in the fieldwork and in the meticulous separation of the Lisan aragonite and detritus laminae from the bulk samples collected in the field. Fruitful discussions with Abraham Starinsky and critical suggestions by two anonymous reviewers significantly contributed to the presentation of this study. Partial research funding was provided by the Israel Science Foundation, grant ISF 694/95 to A.A. and A.K.

Appendix A. Supplementary data

Supplementary data associated with this article can be found, in the online version, at doi:10.1016/j.epsl.2009.06.031.

References

Agnon, A., Migowski, C., Marco, S., 2006. Intraclast breccias in laminated sequences reviewed: Records of paleo-earthquakes. Enzel, Y., A. Agnon M. Stein (eds.), New Frontiers in Dead Sea paleo-environmental research. Geol. Soc. Am. Spec. Pap. 401, 195–214.

Bartov, Y., Stein, M., Enzel, Y., Agnon, A., Reches, Z., 2002. Lake levels and sequence stratigraphy of Lake Lisan, the late Pleistocene precursor of the Dead Sea. Quatern. Res. 57, 9–21.

Bartov, Y., Agnon, A., Enzel, Y., Stein, M., 2006. Late Quaternary faulting and subsidence in the central Dead sea basin. Isr. J. Earth Sci. 55, 17–31.

Begin, Z.B., Ehrlich, A., Nathan, Y., 1974. Lake Lisan, the Pleistocene precursor of the Dead Sea. Geol. Surv. Isr. Bull. 63 30 pp.

Begin, Z.B., Stein, M., Katz, A., Machlus, M., Rosenfeld, A., Buchbinder, B., Bartov, Y., 2004. Southward migration of rain tracks during the last glacial, revealed by salinity gradients in Lake Lisan (Dead Sea rift). Quat. Sci. Rev. 23, 1627–1636.

Begin, Z.B., Steinberger, D.M., Ichinose, G.A., Marco, S., 2005. A 40,000 year unchanging seismic regime in the Dead Sea rift. Geology 33, 257–260.

Bentor, Y.K., 1961. Some geochemical aspects of the Dead Sea and the question of its age. Geochim. Cosmochim. Acta 25, 239–260.

Beyth, M., 1977. Present stage of Dead Sea brines. Geological Survey of Israel, Jerusalem Report MG/11/77. 10 pp.

Brower, E., 1973. Synthesis of barite, celestite, and barium-strontium sulfate solid solution crystals. Geochim. Cosmochim. Acta 37, 155–158.

Chan, L.H., Chung, Y., 1987. Barium and radium in the Dead Sea. Earth Planet. Sci. Lett. 85, 41–53.

Enzel, Y., Kadan, G., Eyal, Y., 2000. Holocene earthquakes inferred from a Fan-Delta sequence in the Dead Sea graben. Quat. Res. 53, 34–48.

Enzel, Y., Agnon, A., Stein, M., 2006. New Frontiers in Dead Sea Paleoenvironmental Research. Geological Society of America Special Paper 401. 253 pp.

Freund, R., Garfunkel, Z., Zak, I., Goldberg, M., Weissbord, T., Derin, B., 1970. The shear along the Dead Sea rift. Philos. Trans. R. Soc. Lond. Ser. A 267, 107–127.

Ganor, J., 1986. Halite islands in the southern basin of the Dead Sea. M.Sc., Hebrew University, Jerusalem. 90 pp.

Ganor, J., Katz, A., 1989. The geochemical evolution of halite structures in hypersaline lakes: The Dead Sea, Israel. Limnol. Oceanogr. 34, 1214–1223.

Garfunkel, Z., 1981. Internal structure of the Dead Sea leaky transform (Rift) in relation to plate kinematics. Tectonophysics 80, 81–108.

Gavrieli, I., Yechieli, Y., Halicz, L., Spiro, B., Bein, A., Efron, D., 2001. The sulfur system in anoxic subsurface brines and its implication in brine evolutionary pathways: the Ca-chloride brines in the Dead Sea area. Earth Planet. Sci. Lett. 186, 199–213.

Goldschmidt, M.J., Arad, A., Neev, D., 1967. The mechanism of saline springs in the Lake Tiberias depression. Geol. Surv. Isr. Bull. 45 19 pp.

Please cite this article as: Katz, A., et al., Earthquake-induced barium anomalies in the Lisan Formation, Dead Sea Rift valley, Israel, Earth Planet. Sci. Lett. (2009), doi:10.1016/j.epsl.2009.06.031

Haase-Schramm, A., Goldstein, S.L., Stein, M., 2004. U-Th dating of Lake Lisan (late Pleistocene Dead Sea) aragonite and implications for glacial East Mediterranean climate change. Geochim. Cosmochim. Acta 68, 985–1005.
Hall, J.K., 1996. Digital topography and bathymetry of the area of the Dead Sea depression. Tectonophysics 266, 177–185.
Heifetz, E., Agnon, A., Marco, S., 2005. Soft sediment deformation by Kelvin Helmholtz instability: a case from Dead Sea earthquakes. Earth Planet. Sci. Lett. 236, 497–504.
Katz, A., Ganor, J., 1985. The genesis of halite structures in the southern basin of the Dead Sea. Research Report, Hebrew University, Jerusalem. 30 pp.
Katz, A., Kolodny, N., 1989. Hypersaline brine diagenesis and evolution in the Dead Sea - Lake Lisan system (Israel). Geochim. Cosmochim. Acta 53, 59–67.
Katz, A., Starinsky, A., 2009. Geochemical history of the Dead Sea. Aquat. Geochem. 15, 159–194.
Katz, A., Kolodny, Y., Nissenbaum, A., 1977. The geochemical evolution of the Pleistocene Lake Lisan-Dead Sea system. Geochim. Cosmochim. Acta 41, 1609–1626.
Ken-Tor, R., Agnon, A., Enzel, Y., Marco, S., Negendank, J.F.W., Stein, M., 2001. High resolution geological record of historic earthquakes in the Dead Sea Basin. J. Geophys. Res. 106, 2221–2234.
Klein-BenDavid, O., Sass, E., Katz, A., 2004. The evolution of marine evaporitic brines in inland basins: the Jordan – Dead Sea Rift valley. Geochim. Cosmochim. Acta 68, 1763–1775.
Klein-BenDavid, O., Gvirtzman, H., Katz, A., 2005. Geochemical identification of fresh water sources in brackish groundwater mixtures; the example of Lake Kinneret (Sea of Galilee), Israel. Chem. Geol. 214, 45–59.
Kolodny, Y., Stein, M., Machlus, M., 2005. Sea-rain-lake relation in the Last Glacial East Mediterranean revealed by $\delta^{18}O$- $\delta^{13}C$ in Lake Lisan aragonites. Geochim. Cosmochim. Acta 69, 4045–4060.
Krumgalz, B., Hecht, A., Starinsky, A., Katz, A., 2000. Thermodynamic constraints on Dead Sea evaporation: can the Dead Sea dry up? Chem. Geol. 165, 1–11.
Krumgalz, B.S., Magdal, E., Starinsky, A., 2002. The evolution of a chloride sedimentary sequence - simulated evaporation of the Dead Sea. Isr. J. Earth Sci. 51, 253–268.
Machlus, M., Enzel, Y., Goldstein, S.L., Marco, S., Stein, M., 2000. Reconstructing low levels of Lake Lisan by correlating fan-delta and lacustrine deposits. Quatern. Int. 73/74, 137–144.
Marco, S., 1996. Paleomagnetism and paleoseismology in the late Pleistocene, Dead Sea graben. Ph.D Thesis, Hebrew University.
Marco, S., Agnon, A., 1995. Prehistoric earthquake deformations near Masada, Dead Sea graben. Geology 23, 695–698.
Marco, S., Agnon, A., 2005. High resolution stratigraphy reveals repeated earthquake faulting in the Masada Fault Zone, Dead Sea transform. Tectonophys 408, 101–112.
Marco, S., Stein, M., Agnon, A., Ron, H., 1996. Long term earthquake clustering: a 50,000 year paleoseismic record in the Dead Sea Graben. J. Geophys. Res. 101, 6179–6192.
Migowski, C., Agnon, A., Bookman, R., Negendank, J.F.W., Stein, M., 2004. Recurrence pattern of Holocene earthquakes along the Dead Sea transform revealed by varve-counting and radiocarbon dating of lacustrine sediments. Earth Planet. Sci. Lett. 222, 301–314.
Migowski, C., Stein, M., Prasad, S., Negendank, J.F.W., Agnon, A., 2006. Holocene climate variability and cultural evolution in the Near East from the Dead Sea sedimentary record. Quatern. Res. 66, 421–431.
Moise, T., Starinsky, A., Katz, A., Kolodny, Y., 2000. Ra isotopes and Rn in brines and ground waters of the Jordan-Dead Sea Rift Valley: enrichment, retardation, and mixing. Geochim. Cosmochim. Acta 64, 2371–2388.
Muir-Wood, R., King, G.C.P., 1993. Hydrological signature of earthquake strain. J. Geophys. Res. 98, 22,035–22,070.
Neev, D., Emery, K.O., 1967. The Dead Sea, depositional processes and environments of evaporites. Geol. Surv. Isr. Bull. 41 147 pp.
Prasad, S., Vos, H., Negendank, J.F.W., Waldmann, N., Goldstein, S.L., Stein, M., 2004. Evidence from Lake Lisan of solar influence on decadal to centennial scale climate variability during marine oxygen isotope stage 2. Geology 32, 581–584.
Sagy, A., Reches, Z., Agnon, A., 2003. Margin architecture of a pull apart basin in 3D: faults, flexures, and joints along the Dead Sea basin. Tectonics 22, 1004.
Schramm, A., 1997. Uranium Series and ^{14}C Dating of Lake Lisan (paleo-Dead Sea) sediments: Implications for ^{14}C time-scale calibration and relation to global paleoclimate. University of Göttigen. 115 pp.
Schramm, A., Stein, M., Goldstein, S.L., 2000. Calibration of the ^{14}C time scale to >40 ka by ^{234}U–^{230}Th dating of Lake Lisan sediments (last glacial Dead Sea). Earth Planet. Sci. Lett. 175, 27–40.
Seilacher, A., 1984. Sedimentary structures tentatively attributed to seismic events. Marine Geol. 55, 1–12.
Stanislavsky, E., Gvirtzman, H., 1999. Basin-scale migration of continental-rift brines: paleohydrologic modeling of the Dead Sea basin. Geology 27, 791–794.
Starinsky, A., 1974. Relationship between Ca-chloride brines and sedimentary rocks in Israel. Ph.D. Thesis. The Hebrew university of Jerusalem, 176 pp.
Stein, M., Starinsky, A., Katz, A., Goldstein, S.L., Machlus, M., Schramm, A., 1997. Strontium isotopic, chemical and sedimentological evidence for the evolution of Lake Lisan and the Dead Sea. Geochim. Cosmochim. Acta 61, 3975–3992.
Stein, M., Starinsky, A., Agnon, A., Katz, A., Raab, M., Spiro, B., Zak, I., 2000. The impact of brine-rock reaction during marine evaporite formation on the isotopic Sr record in the oceans: evidence from Mt. Sedom, Israel. Geochim. Cosmochim. Acta 64, 2039–2053.
Torfstein, A., 2008. Brine-freshwater interplay and effects on the evolution of saline lakes: The Dead Sea Rift terminal lakes. Ph.D., Hebrew University, Jerusalem. 158 pp.
Torfstein, A., Gavrieli, I., Stein, M., 2005. The sources and evolution of sulfur in the hypersaline Lake Lisan (paleo-Dead Sea). Earth Planet. Sci. Lett. 236, 61–77.
Torfstein, A., Gavrieli, I., Katz, A., Kolodny, Y., Stein, M., 2008. Gypsum as a monitor of the paleo-limnological-hydrological conditions in Lake Lisan and the Dead Sea. Geochim. Cosmochim. Acta 72, 2491–2509.
Torfstein, A., Haase-Schramm, A., Waldmann, N., Kolodny, Y., Stein, M., 2009. U-series and oxygen isotope chronology of the mid-Pleistocene Lake Amora (Dead Sea basin). Geochim. Cosmochim. Acta 73, 2603–2630.
Waldmann, N., Starinsky, A., Stein, M., 2007. Primary carbonates and Ca-chloride brines as monitors of a paleo-hydrological regime in the Dead Sea basin. Quat. Sci. Rev. 26, 2219–2228.
Yechieli, Y., Bein, A., 2002. Response of groundwater systems in the Dead Sea Rift Valley to the Nuweiba earthquake: changes in head, water chemistry, and near-surface effects. J. Geophys. Res. 107 (B12), 2332–2341.
Zak, I., 1967. The Geology of Mount Sedom. Ph.D. Thesis, The Hebrew University of Jerusalem, 208 pp.
Zak, I., 1997. Evolution of the Dead Sea brines. In: Niemi, T.M., Ben-Avraham, Z., Gat, J.R. (Eds.), The Dead Sea, The Lake and Its Setting, vol. 36. Oxford University Press, pp. 133–144.
Zilberman-Kron, T., 2008. The origin and evolution of brines in sinkholes along the western shores of the Dead Sea. The Hebrew University of Jerusalem, Jerusalem. 96 pp.

Please cite this article as: Katz, A., et al., Earthquake-induced barium anomalies in the Lisan Formation, Dead Sea Rift valley, Israel, Earth Planet. Sci. Lett. (2009), doi:10.1016/j.epsl.2009.06.031